

Triple-gap superconductivity of MgB_2 - $(\text{La,Sr})\text{MnO}_3$ composite. Which of the gaps is proximity induced?

V. N. Krivoruchko and V. Yu. Tarenkov

*Donetsk Physics & Technology Institute NAS of Ukraine,
Str. R. Luxemburg 72, 83114 Donetsk, Ukraine*

(Dated: February 28, 2022)

Abstract

Interplay of superconductivity and magnetism in a composite prepared of the ferromagnetic half-metallic $\text{La}_{0.67}\text{Sr}_{0.33}\text{MnO}_3$ (LSMO) nanoparticles and the conventional s-wave superconductor MgB_2 has been studied. A few principal effects have been found in bulk samples. With an onset of the MgB_2 superconductivity, a spectacular drop of the sample resistance has been detected and superconductivity has been observed at temperature up to 20K. Point-contact (PC) spectroscopy has been used to measure directly the superconducting energy coupling. For small voltage, an excess current and doubling of the PC's normal state conductance have been found. Conductance peaks corresponding to three energy gaps are clearly observed. Two of these gaps we identified as enhanced Δ_π and Δ_σ gaps originating from the MgB_2 ; the third gap Δ_{tr} is more than three times larger than the largest MgB_2 gap. The experimental results provide unambiguous evidences for a new type of proximity effect which follows the phase coherency scenario of proximity induced superconductivity. Specifically, at low temperature, the p -wave spin-triplet condensate with pairing energy Δ_{tr} is essentially sustained in LSMO but is incapable to display long-range super-current response because of a phase-disordering state. The proximity coupling to MgB_2 restores the long-range phase coherency of the triplet superconducting state, which, in turn, enhances superconducting state of the MgB_2 .

When an itinerant ferromagnet (F) is in contact with an s-wave superconductor (S), superconductivity is expected to decay rapidly (a few nanometers) inside the F owing to the incompatible nature of superconductivity and ferromagnetic order [1]. This expectation was indeed confirmed in various materials and geometries. On the other hand, a series of recent experiments [2–7] present clear evidences that a simple physical interpretation of the proximity effect, reading that the Cooper pairs are broken by a strong exchange field in the F layer, is in reality too simplistic, and an extension of the existing concepts of interplay between superconductivity and ferromagnetism is needed.

From the theoretical viewpoint, a case of an F with a uniform exchange field is well understood and the proximity effect may be described by taking into account the splitting of electronic bands of opposite spins [1]. The situation becomes more complicated if the magnetic structure is inhomogeneous, and only few works (see, e.g. [8]) have been devoted to the problem of superconducting proximity systems with non-collinear magnetic disorder correlated on length scales of an order or larger than the superconducting coherence length. On the other hand, being an experimentally accessible electronic system with tunable parameters, hetero-structures with inhomogeneous magnetism (e.g., superconducting nano-composites) offer a unique testing ground for studying superconducting proximity systems with an arbitrary length of magnetic disorder. However, to our knowledge, up to now no reports have been devoted to a superconductive composite of (nano)granular half-metal ferromagnet (hmF) and a conventional s-wave superconductor.

In our recent works anomalous superconductivity has been detected in point contacts (PCs) of half-metallic manganite, (La,Sr)MnO₃ and (La,Ca)MnO₃, with an s-wave superconductor, Pb or MgB₂, [9, 10]. Particularly, for proximity affected PCs, the coherent multiple Andreev reflection (sub-harmonic gap resonances) has been observed, and it has been found that proximity induced superconducting gap of (La,Sr)MnO₃ or (La,Ca)MnO₃ is much larger than that of the Pb or MgB₂. It was implied that, at low temperature, *non-coherent superconducting fluctuations are essentially sustained in half-metallic manganites and, in proximity affected region, the singlet S establishes phase coherence of the p-wave spin-triplet superconducting state of the manganites* [9, 10]. To verify this phase-disordering scenario for anomalous superconductivity of proximity affected PCs, we prepared and systematically studied normal and superconducting properties of the MgB₂ – (nano) La_{0.67}Sr_{0.33}MnO₃ (MgB:LSMO) composite. The basic idea was to obtain such a composite, where proximity

coupled hmF/S interfaces govern superconducting properties of the sample. Fortunately, the idea was successful, and in this report we present the results of investigating transport properties of such systems. Our key findings are: (i) the samples of MgB:LSMO (nano)composite demonstrate evidences for bulk (triplet) superconductivity with large, up to 20K, critical temperature, T_C ; (ii) three superconducting gaps are clearly observed. We identified two of these gaps as enhanced MgB₂ gaps, the third quasiparticle gap, Δ_{tr} , is more than three times larger than the largest MgB₂ gap and could not be attributed to this superconductor. Also, we found that (iii) all the energy gaps vanish simultaneously as the temperature increases towards T_C of MgB₂.

The origin of the large quasiparticle Δ_{tr} gap and an enhancement of the MgB₂ gaps cannot be explained on the basis of the existing theoretical models. We believe the results obtained are the first observation of the new type of superconducting proximity effect. That is, MgB₂ enhances the internal superconducting order parameter phase stiffness in LSMO and, in turn, being in superconducting state, LSMO enhances superconducting characteristics of MgB₂. Taking into account half-metallic properties of LSMO and the Curie temperature magnitude, we think that in the case of LSMO we deal with even frequency p -wave spin-triplet superconducting pairing.

Experimental details. Stoichiometric MgB₂ has a transition temperature $T_C = 39$ K, the highest among conventional superconductors [11]. MgB₂, however, is by no means an ordinary, but the weakly interacting multiple bands superconductor (σ and π bands). It demonstrates distinct multiple superconducting energy gaps (the σ and π gaps) with energy $\Delta_\pi = 2.3$ meV and $\Delta_\sigma = 7.1$ meV at $T = 4.2$ K [11]. The coherence length ξ is anisotropic with $\xi_{ab}(0) \approx 8$ nm and $\xi_c(0) \approx 2$ nm [11]. La_{0.67}Sr_{0.33}MnO₃ is a hmF with the $T_{Curie} = 320$ K (see, e.g., [12]). Composites containing submicron MgB₂ powder and LSMO particles (about 20nm in size) have been produced. Details of the LSMO nanoparticles preparation may be found in Ref. [13]. The powders with different weight ratios of LSMO and MgB₂ were mixed and pressed (under pressure up to 60 kbar) in stripes, and a number of samples of different composition have been obtained.

The obtained composites were analyzed by the method of X-ray energy-dispersive spectroscopy (EDX) using INCAPentaFETx3 spectrometer and JSM-6490LV scanning electron microscopy (SEM). Exemplarily, one of the sample's SEM micrograph is shown in Fig. 1. Also, AC and DC magnetization measurements were used to study superconducting and

magnetic properties of the samples. In all transport measurements the standard four-point configuration with the low-frequency ac technique was used. The resistance was measured with a current of $\sim 50\mu\text{A}$. For the sample of the same (nominal) composition, sample-to-sample fluctuations in magnitude of the critical temperature and the critical current have been detected.

Experimental results. (i) A representative temperature dependence of the normalized resistivity $R(T)/R(T = 39\text{K})$ of the (bulk) samples with $\text{MgB}_2:\text{La}_{0.67}\text{Sr}_{0.33}\text{MnO}_3$ weight ratio 1:1, 3:1 and 4:1, as well as of the MgB_2 sample without manganite are shown in Fig. 2 (main panel). According to the $R(T)$ dependences, below the superconducting transition temperature of MgB_2 , samples 3:1 and 4:1 resistivity sharply decreases and vanishes at critical temperature $T_C = 20\text{ K}$. The resistivity of sample 1:1 also decreases, but the composite of this composition still remains in a resistive state down to the lowest temperature 4.2K. Sometimes a hysteretic shift in $R(T)$ behavior reflecting the (magnetic) pre-history dependence of the transition temperature was also detected. Below T_C the results for the sample 4:1 basically reproduce those for the composition 3:1, and below we concentrate on the results obtained for samples with weight ratio 3:1.

Figure 3 (main panel) shows the current-voltage ($I - V$) characteristic of the sample 3:1, taken at 4.2K. We observe a clear zero resistance supercurrent branch, with a maximum value for I_C of 2.5 mA. From the $I - V$ characteristics the critical current I_C of the composite was determined as the first deviation from a vertical line around zero bias. The second deviation from linearity around 0.6 mV bias, with a maximum value of 8.9 mA, is attributed to the critical current of the MgB_2 powder. In the current interval $2.5\text{ mA} < I < 8.9\text{ mA}$ the sample is in a resistive state and could be considered as a system of small superconductive islands within a normal matrix. For comparison, in Fig. 3 (inset) the $I - V$ characteristic of sample 1:1 at 4.2K is also shown. This system remains in a resistive state, however, an excess current has been clearly observed. Formally, the system is similar to arrays of resistively shunted Josephson junctions.

The 3:1 composite magnetic susceptibility χ and magnetization M plotted as temperature $\chi(T)$ and field $M(H)$ dependences are shown in Fig. 4 (a) and Fig. 4 (b), respectively. As follows from the data for $\chi(T)$ in Fig 4 (a), with decreasing temperature, a transition into ferromagnetic state occurs with $T_{Curie} = 320\text{ K}$ and then, below 39K, a diamagnetic response is developed. The measured magnetization hysteresis loop [see Fig.4 (b)] provides

the unambiguous evidence that our composite is a type-II superconductor with a strong vortex pinning. At low temperature, with increasing an applied field, a diamagnetic response is suppressed and above 3.3 kOe a ferromagnetic response is again restored due to flux penetration and magnetization of the sample.

(ii) Point-contact spectroscopy allows a direct measurement of the superconducting gap. Figure 5 shows representative spectra of In, Ag, Nb – sample 3:1 PCs measured at $T = 4.2$ K. We underline that the PCs' resistivity varied by order, but multiple gaps structure in the quasiparticle density of states of the composite, as well as the gap energy magnitudes were robust features of superconducting composites and were reproduced in all PCs we prepared. Conductance peaks corresponding to three superconducting gaps with energies $\Delta_1(\pi) = 2.0 \div 2.4$ meV, $\Delta_2(\sigma) = 8.4 \div 11.7$ meV, and $\Delta_{tr} = 19.8 \div 22.4$ meV are clearly observed. Here we will adopt abbreviation $\Delta_1(\pi)$ and $\Delta_2(\sigma)$ for gaps which originate (most probably) from the Δ_π and Δ_σ gaps of MgB_2 , respectively, and Δ_{tr} which we attribute (see discussion below) to the superconductivity of LSMO. It is worth underlining here that magnitude of Δ_{tr} is the same as those earlier detected in PCs of $(\text{La,Sr})\text{MnO}_3$ and $(\text{La,Ca})\text{MnO}_3$ with Pb or MgB_2 [9, 10]. In Fig. 6, the energy gap Δ_{tr} temperature dependence is shown. From the BCS relation $\Delta(0) = 1.76k_B T_C$, the $\Delta_{tr}(0)$ gap would lead to a S with $T_C \approx 120$ K. The classic BCS gap temperature behavior is shown in the figure too. As is evident, the experimental data does not follow the BCS dependence.

Thus, principal features which arise from the data obtained in all PCs are (i) a triple-gap structure of the PCs spectra; (ii) the *enhanced* MgB_2 gaps. (Note, to avoid confusion, that within the accuracy of our measurements, the magnitude of the $\Delta_1(\pi)$ gap still remains in range of a bulk MgB_2 Δ_π gap [11].) Also, (iii) proximity induced quasiparticle gap Δ_{tr} is more than three times larger than the conventional Δ_σ gap of MgB_2 .

Discussion. Here we will concentrate on temperature region $T < T_C$ and superconducting state of the 3:1 and 4:1 samples. As already mentioned, an origin of the large quasiparticle Δ_{tr} gap and an enhancement of the largest MgB_2 gap, Δ_σ , cannot be conventionally explained on the basis of the existing theoretical models of proximity effect. Theoretically, the proximity effect in normal metal – multi-band (MgB_2) hybrid structures has been considered by Brinkman *et al.*, [14]. A phenomenon was predicted, where the superconductivity in a two-band superconductor is enhanced by the proximity to a superconductor with a lower transition temperature (S'). The physics of this effect is explained by the coupling between S'

and the π -band: S' superconductor enhances the superconductivity in the π -band, whereas the $\pi - \sigma$ interband coupling causes an enhancement of the superconductivity in the σ -band. However, for MgB:LSMO composite we found three quasiparticle gaps, the largest of which, Δ_{tr} , could not be attributed to MgB₂. Also, a substantial increase in the magnitude of the largest of MgB₂ gap, Δ_{σ} , has been detected. Thus, a question arises as to which of these gaps is proximity induced?

Before giving a qualitative explanation of the observations, we summarize the physics of proximity effect at spin-active hmF/S interface which looks as follows (see, e.g., [15] and references therein). The conversion process between the singlet and equal-spin triplet supercurrents is believed to be governed by two important phenomena taking place in the half metal at the interface: (i) a spin mixing and (ii) a spin-rotation symmetry breaking. Spin mixing is the result of different scattering phase shifts that electrons with opposite spin acquire when scattered (reflected or transmitted) from an interface. It results from either a spin-polarization of the interface potential, or differences in the wave-vector mismatches for spin up and spin down particles at either side of the interface, or both. It is a robust and ubiquitous feature for interfaces involving strongly spin-polarized ferromagnets.

Broken spin-rotation symmetry leads to spin-flip processes at the interfaces. Its origin depends on microscopic magnetic state at the hmF/sS interface, character of local magnetic moments coupling with itinerant electrons, etc., and even varies from sample-to-sample. However, the exact microscopic origin of spin-flip processes at the interface is important only for the effective interface scattering matrix [15] and not for superconducting phenomena, since Cooper pairs are of the size of the coherence length ξ which is much larger than the atomic scale.

Due to spin mixing at the interfaces, a spin triplet ($S = 1, m = 0$) amplitude, $f_{\uparrow\downarrow}^{tr}(r) = (|\uparrow\downarrow\rangle + |\downarrow\uparrow\rangle)$, is created and extends from the interface about a length $\xi_F = (D_F/2\pi H_{exc})^{1/2}$ into the F layer (D_F denotes the diffusion constant in the F). At the same time, triplet pairing correlations with equal spin pairs ($S = 1, m = +1$ or $m = -1$) are also induced (due to spin-flip processes) in the F layer. These components decay on the length scale $\xi_T = (D_F/2\pi T)^{1/2}$ which is much larger than ξ_F because in typical cases exchange field H_{exc} is much larger than T_C . It is worth emphasizing that it is only the $m = 0$ triplet component that is coupled via the spin-active boundary condition to the equal-spin $m = 1$ pairing amplitudes in the half-metal. The singlet component in the superconductor,

$f_{\uparrow\downarrow}^s(r) = (|\uparrow\downarrow\rangle - |\downarrow\uparrow\rangle)$, being invariant under rotations around any quantization axis, is not directly involved in the creation of the triplet $m = 1$ pairing amplitudes in the half-metal.

Note, that for odd-frequency s -wave spin-triplet pairing [16] the static gap is zero. We observe nonzero gaps magnitudes, and thus this scenario of proximity effect is not related to our case.

We now proceed to our system. Within the double-exchange interaction model for hole-doped manganites (see, e.g., [12]), the itinerant charge carriers provide both the magnetic interaction between magnetic moments of the nearest Mn^{3+} - Mn^{4+} ions and the system's electrical conductivity. Due to the short mean free path, that is typically the distance of about a lattice parameter, the charge carrier probes the magnetization on a very short length scale. At the interfaces with the superconductor, the local moments are expected to show a certain degree of disorder and it is reasonable to expect that the interface ferromagnetic manganite - s -wave S is a spin-active one. (Note also that local magnetic structure at the hmF/sS interface can be easily affected by an external influence that leads to hysteretic behavior of the equilibrium properties as we indeed observe in some cases.) Following to Refs.[9, 10], we suggest that, at low temperature, non-coherent p -wave even-frequency spin-triplet superconducting condensate already exists in half-metallic manganites. Being proximity coupled to the singlet superconductor, the $m = 0$ triplet component in the hmF is coupled via boundary condition to the singlet pairing amplitude in the S partner. At the same time, the spin-active boundary leads to coupling of the $m = 0$ triplet component with an equal spin $m = 1$ pairing amplitude in manganite. These couplings yield phase-coherency of both $m = 0$ and equal-spin triplet Cooper pairs in the hmF with large quasiparticle gap Δ_{tr} ($> \Delta_{\pi}, \Delta_{\sigma}$). As an inverse effect, being proximity linked to s -wave pairing amplitude, the $m = 0$ amplitude of the triplet superconducting state enhances the quasiparticle gap(s) of a singlet superconductor.

It is worthy to note here that in mean field BCS-Eliashberg theories, the temperatures of electron-pairing, T_{Δ} , and the long-range phase coherency, T_{φ} , coincide and yield the critical temperature, T_C . This means that the global phase coherency and energy gap appear/vanish at the same temperature, mainly due to the opening/disappearing of the gap with temperature (i.e., the relation $T_{\varphi} > T_{\Delta}$ is a typical case). However, it has been shown [17] (see also [18]) that for systems with low conductivity and small super-fluid density (bad metals), the temperature of the global phase coherency T_{φ} is reduced significantly

and becomes comparable to or even smaller than the pairing temperature T_{Δ} . In this case, the critical temperature T_C is determined by the global phase coherency, whereas the pair condensate could exist well above T_C . The experimental results shown in Fig. 6 support the picture where the metastable superconducting islands of nonzero order parameter are frozen, while the long-range coherence associated with a bulk superconducting state is prevented by marked fluctuations in the phase. (The loss of long-range phase stiffness, rather than the vanishing of the pair condensate well above T_C , is at present actively discussed in relation to several families of hole-doped cuprates; see, e.g. [19, 20] and references therein.)

The important consequence of the presence of the Cooper pair fluctuation above T_C is an appearance of the so-called pseudo-gap [17, 21, 22], i.e., decreasing of the one-electron density of state near the Fermi level. A large pseudo-gap is indeed detected in numerous experiments on manganites [12] and it may be suggested that at least a portion of the observed pseudo-gap is due to pairing without global phase coherency. Diamagnetic response above T_C provides additional arguments for survival of the pair condensate well above T_C in cuprates [19] as well as in disordered MgB_2 [23] and oxy-pnictides [24]. However, for manganites this kind of response will be strongly suppressed by ferromagnetic order of the localized moments and spin-triplet state of the condensate.

Summary. We produced and studied magnetic and superconducting properties of $\text{MgB}_2 - (\text{nano}) \text{La}_{0.67}\text{Sr}_{0.33}\text{MnO}_3$ composite. Unconventional superconductivity of samples $\text{MgB}:\text{LSMO}$ with 3:1 and 4:1 weight ratio with $T_C = 20$ K has been observed. Three distinct quasiparticle energy gaps $\Delta_1(\pi)$, $\Delta_2(\sigma)$, and Δ_{tr} are clearly revealed. Two of these gaps were identified as gaps originating from the MgB_2 . The third gap Δ_{tr} , which is a few times larger than the largest MgB_2 gap, could not be attributed to this s -wave superconductor. In our opinion, the results obtained testify in favor of the induced long-range phase coherency of p -wave even frequency spin triplet superconductivity of half-metallic $\text{La}_{0.67}\text{Sr}_{0.33}\text{MnO}_3$. Specifically, in a ferromagnetic state of $\text{La}_{0.67}\text{Sr}_{0.33}\text{MnO}_3$, a condensate lost phase stiffness and is incapable to display long-range supercurrent response, even though the gap amplitude is large. Nonetheless, reduced local phase rigidity survives. Being proximity coupled to MgB_2 , the long-range coherency is restored. An inverse effect of the proximity induced superconducting state with large gap is an enhancement of the MgB_2 superconducting state. I.e., here we deal with some kind of "mutual" proximity effect.

The authors acknowledge I. A. Danilenko for the LSMO nanoparticles preparation. We

also are grateful to M. Kupriyanov, Ya. Fominov for useful discussions, and M. Belogolovskii for helpful comments on the manuscript.

-
- [1] A.I. Buzdin, Rev. Mod. Phys. **77**, 935 (2005).
 - [2] M. Giroud, H. Courtois, K.Hasselbach, D. Mailly, and B. Pannetier, Phys. Rev. B **58**, R11872 (1998).
 - [3] V. T. Petrashov, I. A. Sosnin, I. Cox, A. Parsons, and C. Troadec, Phys. Rev. Lett. **83**, 3281 (1999).
 - [4] V. Peña, Z. Sefrioui, D. Arias, C. Leon, J. Santamaria, M. Varela, S. J. Pennycook, and J. L. Martinez, Phys. Rev. B **69**, 224502 (2004).
 - [5] I. Sosnin, H. Cho, V. T. Petrashov, and A. F. Volkov, Phys. Rev. Lett. **96**, 157002 (2006).
 - [6] R. S. Keizer, S.T.B. Goennenwein, T.M. Klapwijk, G. Maio, G. Xiao, and A. Gupta, Nature (London) **439**, 825 (2006).
 - [7] J. Wang, M. Singh, M. Tian, N. Kumar, B. Liu, C. Shi, J.K. Jain, N. Samarth, T.E. Mallouk, and M.H.W. Chan, Nature Physics **6**, 389 (2010).
 - [8] D. A. Ivanov, Ya. V. Fominov, M. A. Skvortsov, and P. M. Ostrovsky, Phys. Rev. B **80**, 134501 (2009).
 - [9] V. N. Krivoruchko, V. Yu. Tarenkov, A. I. D'yachenko, and V. N. Varyukhin, Europhys. Lett. **75**, 294 (2006).
 - [10] V. N. Krivoruchko and V. Yu. Tarenkov, Phys. Rev. B **75**, 214508 (2007); *ibid.* **78**, 054522 (2008).
 - [11] X. X. Xi, Rep. Prog. Phys. **71**, 116501 (2008).
 - [12] E. Dagotto, T. Hotta, and A. Moreo, Phys. Rep. **344**, 1 (2001).
 - [13] M.M. Savosta, V. N. Krivoruchko, I. A. Danilenko, V. Yu. Tarenkov, T.E. Konstantinova, A. V. Borodin, and V. N. Varyukhin, Phys. Rev. B **69**, 024413 (2004); V. Krivoruchko, T. Konstantinova, A. Mazur, A. Prokhorov, V. Varyukhin, J. Magn. Magn. Mater. **300**, e122 (2006).
 - [14] A. Brinkman, A. A. Golubov, and M. Yu. Kupriyanov, Phys. Rev. B **69**, 214407 (2004).
 - [15] M. Eschrig, J. Kopu, J. C. Cuevas, and G. Schön, Phys. Rev. Lett. **90**, 137003 (2003); M. Eschrig and T. Löfwander, Nature Phys. **4**, 138 (2008).

- [16] F.S. Bergeret, A.F. Volkov, and K.B. Efetov, Phys. Rev. Lett. **86**, 4096 (2001).
- [17] V. J. Emery and S.A. Kivelson, Phys. Rev. Lett. **74**, 3253 (1995).
- [18] E. Berg, D. Orgad, and S. A. Kivelson, Phys. Rev. B **78**, 094509 (2008).
- [19] Lu Li, Y. Wang, S. Omiya, S. Ono, Y. Ando, G. D. Gu, and N. P. Ong, Phys. Rev. B **81**, 054510 (2010).
- [20] L.S. Bilbro, R.V. Aguilar, G. Logvenov, O. Pelleg, I. Bozovic, and N.P. Armitage, Nature Phys. **7**, 298 (2011).
- [21] V.M. Loktev, R.M. Quick, and S.G. Sharapov, Phys. Rep. **349**, 1 (2001).
- [22] M. Norman, D. Pines, and C. Kallin, Adv. Phys. **54**, 715 (2005).
- [23] E. Bernardi, A. Lascialfari, A. Rigamonti, and L. Romanò, Phys. Rev. B **77**, 064502 (2008).
- [24] G. Prando, A. Lascialfari, A. Rigamonti, L. Romanò, S. Sanna, M. Putti, and M. Tropeano, Phys. Rev. B **84**, 064507 (2011).

Figure Captions

Fig. 1. SEM image of $\text{MgB}_2:\text{La}_{0.67}\text{Sr}_{0.33}\text{MnO}_3$ composite with 3:1 weight ratio (black – MgB_2 , light tone - $\text{La}_{0.67}\text{Sr}_{0.33}\text{MnO}_3$).

Fig. 2 Temperature dependence of the normalized resistivity $R(T)/R(T = 39\text{K})$ of the samples with $\text{MgB}_2:\text{La}_{0.67}\text{Sr}_{0.33}\text{MnO}_3$ weight ratio 1:1, 3:1 and 4:1, as well as of pure (weight ratio 1:0) MgB_2 . *Inset*: samples resistivity at $T = 300\text{K}$.

Fig. 3. (a) Current-voltage characteristic of $\text{MgB}_2:\text{La}_{0.67}\text{Sr}_{0.33}\text{MnO}_3$ (3:1) sample. (b) Current-voltage characteristic of $\text{MgB}_2:\text{La}_{0.67}\text{Sr}_{0.33}\text{MnO}_3$ (1:1) sample.

Fig. 4. (a) Temperature dependence of the magnetic susceptibility of $\text{MgB}_2:\text{La}_{0.67}\text{Sr}_{0.33}\text{MnO}_3$ (3:1) sample. *Inset*: high temperature region. (b) Magnetization $M(H)$ curves of $\text{MgB}_2:\text{La}_{0.67}\text{Sr}_{0.33}\text{MnO}_3$ (3:1) sample and MgB_2 .

Fig. 5. The spectra of In – sample 3:1, Ag – sample 3:1 and of Nb – sample 3:1 point contacts.

Fig. 6. Gap $\Delta_{tr}(T)$ values (relative to zero temperature gap) of $\text{MgB}_2:\text{La}_{0.67}\text{Sr}_{0.33}\text{MnO}_3$ (3:1) composite as function of temperature and the BCS gap temperature dependence.

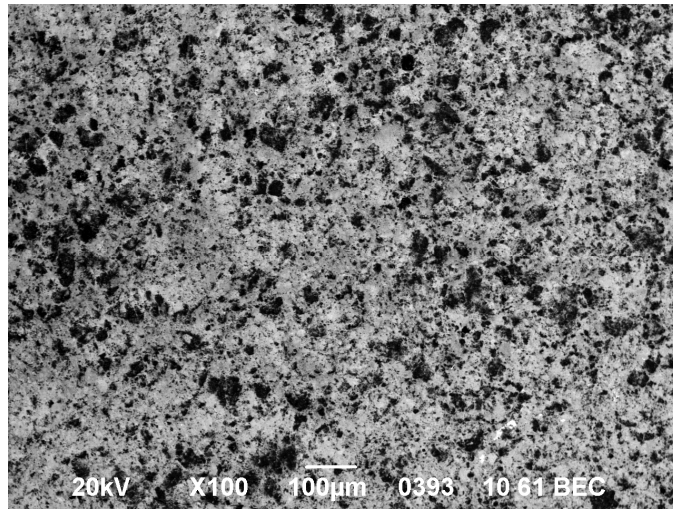


Fig. 1.
SEM image of $\text{MgB}_2:\text{La}_{0.67}\text{Sr}_{0.33}\text{MnO}_3$ composite with 3:1 weight ratio (black – MgB_2 , light tone - $\text{La}_{0.67}\text{Sr}_{0.33}\text{MnO}_3$).

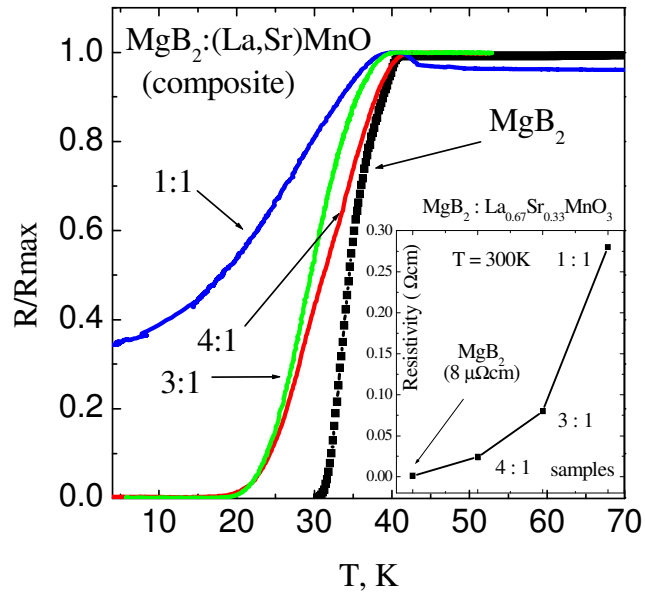


Fig. 2
 Temperature dependence of the normalized resistivity $R(T)/R(T = 39\text{K})$ of the samples with $\text{MgB}_2:\text{La}_{0.67}\text{Sr}_{0.33}\text{MnO}_3$ weight ratio 1:1, 3:1 and 4:1, as well as of pure (weight ratio 1:0) MgB_2 .
Inset: samples resistivity at $T = 300\text{K}$.

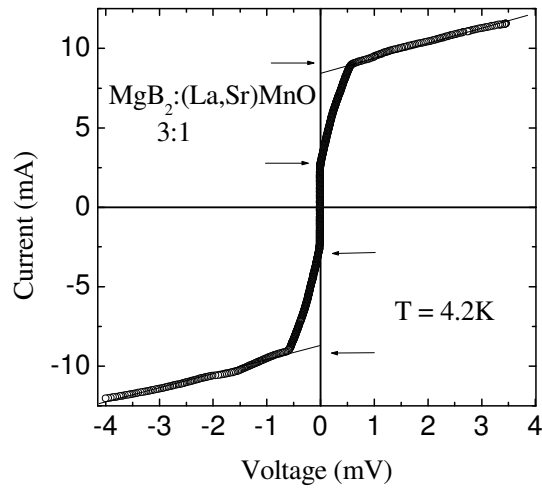


Fig. 3 (a)
Current-voltage characteristic of the $\text{MgB}_2:\text{La}_{0.67}\text{Sr}_{0.33}\text{MnO}_3$ (3:1) sample.

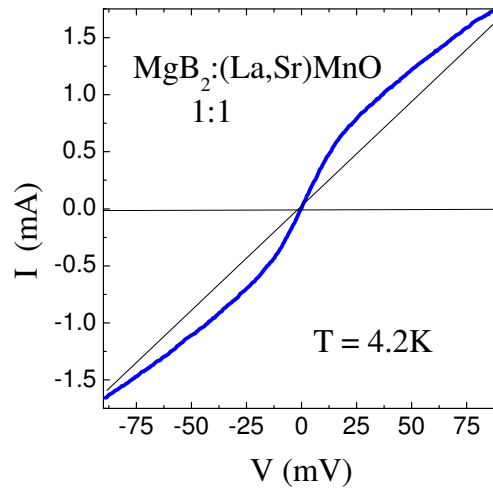


Fig.3 (b)
Current-voltage characteristic of the $\text{MgB}_2:\text{La}_{0.67}\text{Sr}_{0.33}\text{MnO}_3$ (1:1) sample.

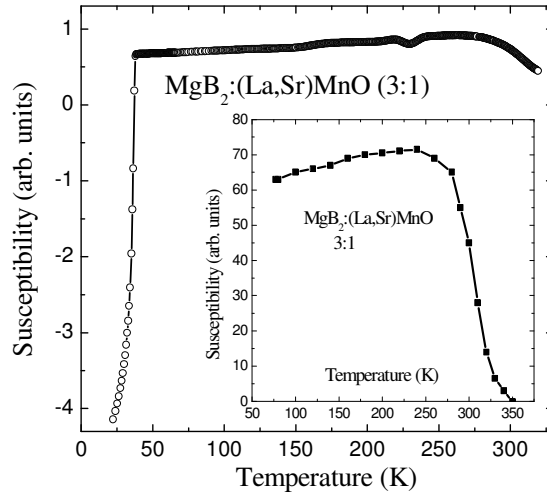


Fig. 4 (a)
 Temperature dependence of the magnetic susceptibility of $\text{MgB}_2:\text{La}_{0.67}\text{Sr}_{0.33}\text{MnO}_3$ (3:1) sample.
Inset: high temperature region.

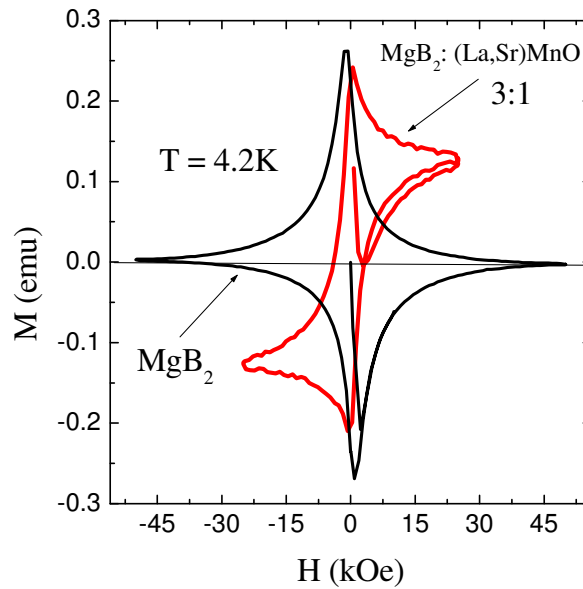


Fig. 4 (b)
 Magnetization $M(H)$ curves of $\text{MgB}_2:\text{La}_{0.67}\text{Sr}_{0.33}\text{MnO}_3$ (3:1) sample and MgB_2 .

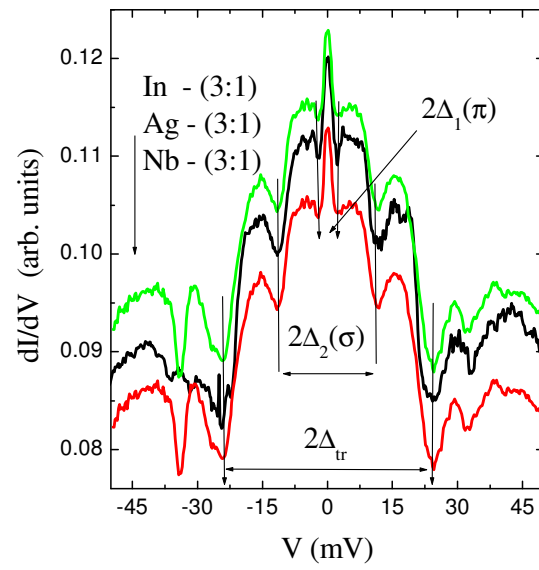


Fig. 5. The spectra of In - sample 3:1, Ag - sample 3:1 and of Nb - sample 3:1 point contacts.

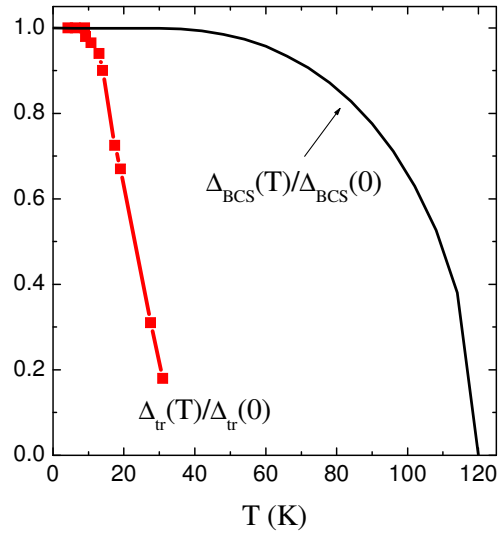


Fig. 6
 Gap $\Delta_{tr}(T)$ values (relative to zero temperature gap) of Nb - MgB₂:La_{0.67}Sr_{0.33}MnO₃ (3:1) composite as function of temperature and the BCS gap temperature dependence.